Carbonates and Evaporites (2024) 39:24
https://doi.org/10.1007/s13146-024-00951-8

ORIGINAL ARTICLE

A detailed investigation of Jutana Formation for depositional setting in Indus Basin, Pakistan

Muhammad Ibrar[2] · Hameed Ur Rehman[3] · Suleman Khan[3] · Syed Saddam Hussain[3] · Maqsood Ur Rahman[1] · Abdullah Khan[4]

Accepted: 22 February 2024 / Published online: 4 March 2024

Abstract

The origin and depositional setting of dolomites remain a complex and debated topic. In the Indus Basin Pakistan, the dolomites in Jutana Formation form a thick sequence within the Cambrian stratigraphy. The current study investigates the detailed depositional setting as well as the mineralogical composition of dolomites in the Jutana Formation to provide insight into their origin. The study focuses on integrating the microfacies and Scanning Electron Microscopy (SEM) with X-ray diffraction (XRD) data along with Wireline logs of Jutana Formation in Khewra Gorge, Eastern Salt Range. Based on field and petrographic observations, four microfacies were identified including (a) siliciclastic algal laminated dolomitic breccia (MJD-1), (b) burrowed sandy ferroan dolomicrite (MJD-2), (c) in-situ medium-coarse grained dolomicrite-dolosparite (MJD-3), (d) fine grained micaceous dolosparite (MJD-4). The microfacies analysis reveals that the deposition of the Jutana Formation is primary on carbonate platform in peritidal environments, ranging from supratidal to subtidal. Digenesis has obliterated most of the primary depositional features, making the interpretation of the original depositional setting challenging. The XRD analysis suggests that these dolomites are nearly stoichiometric and less ordered, indicating an early diagenetic setting, further supported by the presence of anhydrite seen under the SEM. The original depositional setting on the carbonate platform is also supported by cross plot graph wireline logs.

Keywords Cambrian · Microfacies · Diagenesis · XRD · Well logs

✉ Maqsood Ur Rahman
maqsood@cug.edu.cn

Muhammad Ibrar
mibrar@uswat.edu.pk

Suleman Khan
sulemanafridi2004@yahoo.com

Syed Saddam Hussain
Syed.geo99@gmail.com

Abdullah Khan
abdullahkhanwazir@cug.edu.cn

1 Institute for Advanced Marine Research, China University of Geosciences, 511462, Guangzhou, China

2 Centre for Earth & Space Sciences, University of Swat, Swat, Pakistan

3 Department of Geology, University of Peshawar, Peshawar 25120, Pakistan

4 State Key Laboratory of Biogeology and Environmental Geology, China University of Geosciences, Wuhan 430074, China

Introduction

Dolomite (Ca Mg $(CO_3)_2$) is abundant in the Pre-Cambrian formations but is noticeably rare in modern sedimentary environments. It is one of the essential components of dolostones and marlstones as widely found in carbonate sedimentary formations (Lippmann and Lippmann 1973; Land 1985; Gregg et al. 2015; Pina et al. 2020). A substantial body of experimental research and calculations suggests these dolomite formations may unfold through various stages of replacement and recrystallization(Given and Wilkinson 1987; Warren 2000). The dolomitization is a complex phenomenon which can occur through various mechanisms, including diagenetic alteration, hydrothermal processes, microbial activity, and seawater evaporation (e.g., Warren 2000; Gregg et al. 2015). Several studies proposed the idea of early-stage diagenetic process after the deposition in which the sea water provide the Mg content. The sabkha model is one of the proposed theories, suggesting that the initial diagenetic transformation of calcite or aragonite precursors to dolomite occurs at temperatures below 60 °C in evaporative environments, such as hypersaline ponds associated with sabkhas (Warren 2000; Yong-quan et al. 2008; You et al. 2018). This transformation is believed to be caused by the reflux of magnesium-rich sea waters (Land 1985; Warren 2000). Another suggested mechanism is the organogenic dolomite model, which involves the direct precipitation of high-Mg calcite and either nonstoichiometric or stoichiometric dolomite from seawater or near-surface pore waters due to microbial-organic processes (Vasconcelos et al. 1995; Qiu et al. 2017). However, the origin and the depositional setting of dolomites are still subjects of debate and unresolved issues.

is In the Indus Basin, Pakistan, dolomitic beds in the Kingriali, Samana Suk, and Kawagarh formations are believed to have diverse origins (Ahmad et al. 2013; Rahman et al. 2016, 2017; Shah et al. 2016; Khan and Shah 2019). Similarly, the Jutana Formation in the Upper Indus Basin contains substantial dolomitic bodies, presumed by Ahmad et al. (2013) to be of primary origin whereas Khan and Shah (2019) linked to multi stages dolomitization. However, insufficient attention has been given to the depositional setting of the Jutana Formation, which is crucial for understanding the origin of the various lithofacies, including dolostone. This study aims to investigate the Jutana Formation in the Kewra Gorge Section of the Upper Indus Basin (Fig. 1), in order to provide a comprehensive analysis of its depositional setting and diagenesis. Our approach integrates outcrop data, petrographic observations, X-ray Diffraction (XRD) analysis, SEM (Scanning Electron Microscopy) imaging, and wireline logs to distinguish the fine crystalline nature of the Jutana Formation dolomites within their environmental context. Through this comprehensive investigation, our study aims to offer detailed insights into the depositional model and post-depositional diagenesis processes.

Regional Geology

The subduction of the Indian Plate beneath the Eurasian Plate has led to the emergence of several prominent tectonic features in the northern and northwestern peripheries of the Indian Plate. As a consequence of this subduction, the formation of the Himalayan mountain ranges and a series of foreland fold-and-thrust belts occurred (Kazmi and Jan 1997). The northward subduction of the Indian Plate represents the principal tectonic framework of northern Pakistan, encompassing significant structures such as the Main Karakorum Thrust (MKT), Main Mantle Thrust (MMT),

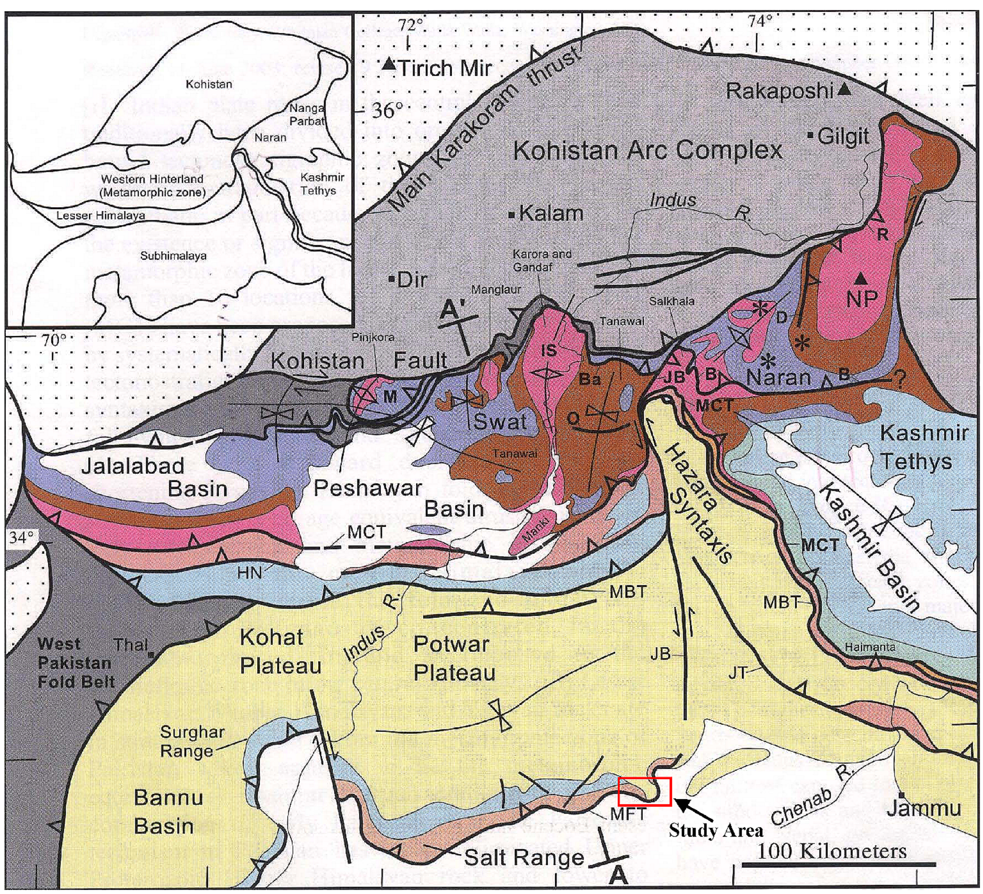

Fig. 1 The Generalized tectonic map of northwestern Pakistan showing major tectonic elements (after Kazmi and Rana (1982)

Main Boundary Thrust (MBT), and the Salt Ranges Thrust (SRT) (Fig. 1). The SRT is positioned as the southernmost thrust zone along the foothills of the Salt and Trans-Indus Ranges which is largely covered by Quaternary alluvium and conglomerates (Kazmi and Jan 1997). However, in some regions, the thrust exposed the area where Paleozoic rocks overlay Neogene or Quaternary deposits in the Jhelum Plain (Gee 1945). In the Salt Range, the stratigraphic units range from the Precambrian to the Recent era, with the Ordovician, Silurian, Devonian, and Carboniferous strata notably absent across the region. The stratigraphic sequence in the Salt Range laterally pinches out, with a well-developed Mesozoic sequence observable in the Western Salt Range and the Trans Indus Ranges, whereas Triassic and Cretaceous strata are missing in the Central and Eastern Salt Range (Shah 1977).

In the Cambrian era, the study area was a portion of the Gondwanaland, that underwent warm, shallow marine depositional conditions (Kadri 1995; Kazmi and Jan 1997). During this era, clastics, evaporites and limestone deposition occurred in lagoon and shallow marine environments (Kadri 1995). The Cambrian strata in the study area (eastern Salt Ranges) encompass the Jhelum Group, consisting of the Khewra Sandstone, Kussak, Jutana, and Baghanwala formations. In a conformable sequence, the Khewra Sandstone lies above the Salt Range Formation of the Pre-Cambrian age and below the Kussak Formation. The Kussak Formation exhibits a conformable upper contact with the Jutana Formation which in turn conformably underlies the Baghanwala Formation. The Jutana Formation predominantly comprises dolomite and is subdivided into three distinct units (Khan et al. 1977): (a) Lower dolomite unit exhibits a light cream to grey color, and is characterized by arenaceous and micaceous impurities, notably interspersed with calcareous sandstone intercalations. It exhibits a massive structure, well-defined bedding, and channelized beds. Additionally, thin clay intercalations are sporadically distributed. Throughout various stratigraphic levels, trough cross-bedding is prominently observed. (b) Middle shale unit located below the glauconitic sandstone. It consists of a thick layer of dark bluish-grey and maroon-colored shale and siltstone which is further succeeded by maroon siltstone and sandstone. This shale layer exhibiting features similar to those of the Kussak Formation. It is highly fossiliferous which has similarities with the Kussak Formation's fossils (Schindewolf and Seilacher 1955). (c) The upper dolomite unit displays light cream to whitish color, characterized by high hardness and massive nature. The bedding is notably thicker compared to the lower dolomite unit and has sand and micaceous impurities. Moreover, it is extensively jointed and fractured and has numerous stylolites. The middle part of the upper unit shows brecciation which is probably caused by contemporaneous deformation (Khan et al. 1977). Notably, trace fossils, particularly tracks and burrows of trilobites, have been documented by Schindewolf and Seilacher (1955). Conformable lower and upper contacts of the Jutana Formation with the Kussak Formation and Baghanwala Formations have been marked.

Materials and methods

The 30 meters thick stratigraphic unit of the Jutana Formation was logged and collected 25 samples for laboratory analysis (Fig. 2). The thin sections were prepared for petrographic studies at the rock cutting laboratory of the Department of Geology, University of Peshawar. The petrographic analysis was performed with an Olympus compound microscope (Model Bx 51) and microphotographs were taken with an Olympus Digital Camera (Model C-5000) by using objectives of X_4, X_{10} and X_{40} magnifications. The microfacies of the dolomite were developed using the standard classification systems outlined by Sibley and Gregg (1987) and Friedman and Sanders (1967), which consider crystal size, texture, fabric, distribution, and shape. Subsequently, the data obtained from these observations were presented and recorded in accordance with the visual comparison charts established by Baccelle and Bosellini (1965).

Seven representative samples were selected for XRD analysis, conducted at the Centralized Resource Laboratory (CRL), Department of Physics, University of Peshawar, in combination with SEM. The interpretation of XRD analysis results have been made using Table 1. The XRD charts show the intensity values on y-axis and 2θ values on the x-axis. The d_{104} peak value offers molar concentration data. The molar concentration was determined by using Lumsden equation. Additionally, major and minor peak values were derived from the XRD data, enabling the determination of the molar concentration of $CaCO_3$, and establishing the ordering for the dolomites of Jutana Formation. The data calculated by using the Lumsden equation is represented in the Table 2. Furthermore, wireline data from the abandoned well Turkwal-01 was sourced from the Director General Petroleum Concession (DGPC), with the wireline logging activities executed by Landmark Resources (LMKR). The log suite encompassed resistivity (LLD) logs, SP logs, gamma ray (GR) logs, bulk density (RHOB) logs, neutron porosity (PHIN) logs, sonic (DT) logs, and photoelectric effect (PEF) logs. Finally, an integrated approach was employed to interpret all the acquired data.

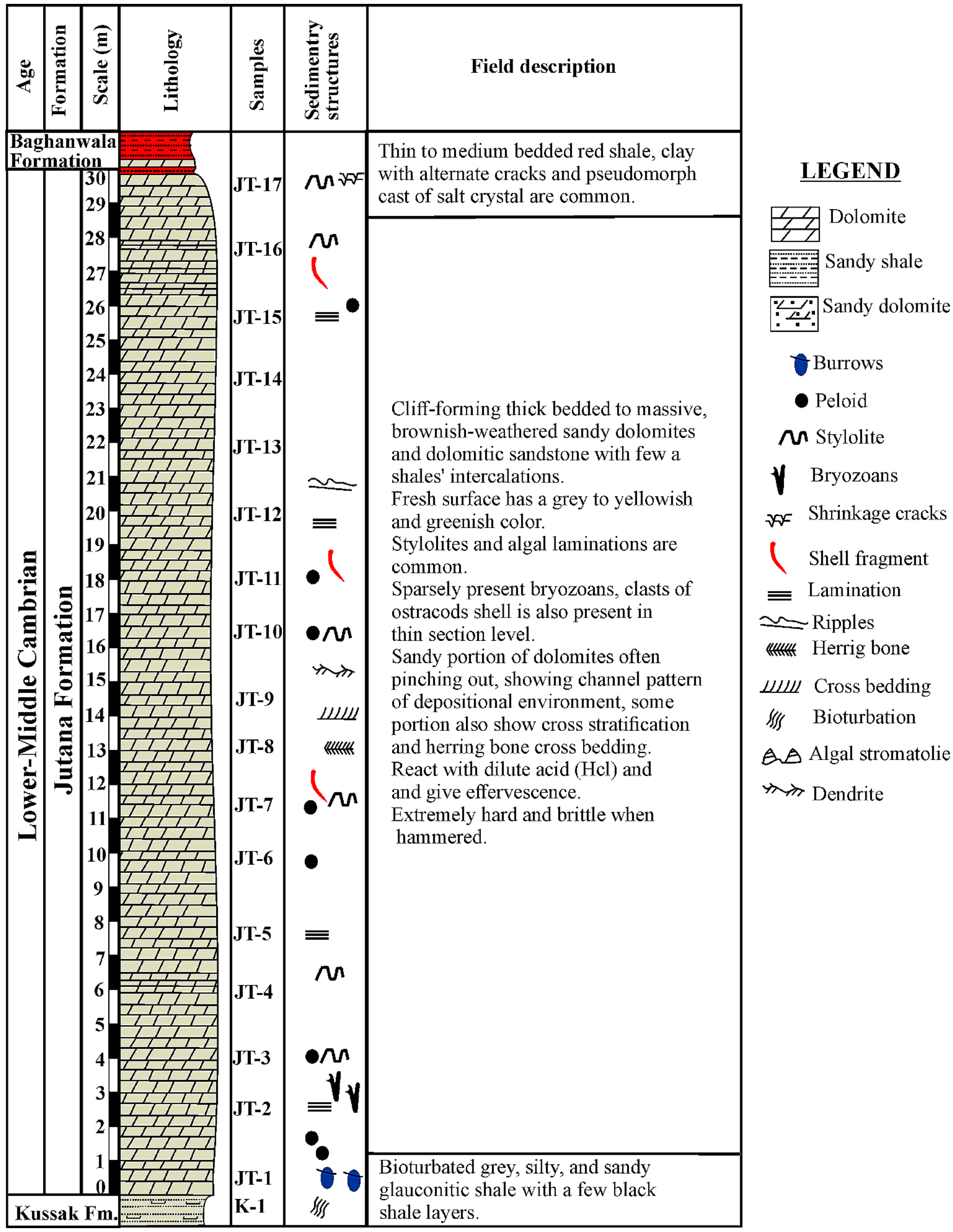

Fig. 2 The stratigraphy of Jutana Formation, Central Salt Range, Upper Indus Basin Pakistan

Results

Microfacies types

Based on petrographic observation four microfacies were identified including: (a) siliciclastic algal laminated dolomitic breccia (MJD-1), (b) burrowed sandy ferroan dolomicrite (MJD-2), (c) in-situ medium-coarse grained dolomicrite-dolosparite (MJD-3) and (d) fine grained micaceous dolosparite (MJD-4). The detailed description is provided below.

Siliciclastic algal laminated dolomitic breccia (MJD-1)

In the outcrop, the rocks consist of medium to thick-bedded, highly porous sandy dolostone displaying light brown to brownish grey colors. Petrographically, the rocks are dominantly composed of fine-dolomite rhombs mixed with quartz. Moreover, the Birdseye structure is common in this microfacies. The dolomite rhombs are anhedral to subhedral, with non-planar boundaries and are loosely packed. The clastic input is observed throughout the microfacies, which is mostly distributed throughout the growth of algal laminations (Fig. 4a–b). The quartz grains constitute about 8–10% of the whole composition whereas in some portions

Table 1 The XRD data of selected samples and the matching pdf sets of standard JCPDS-ICPD diffraction patterns

JT15		JT16		JT17		JT1		PDF# 11–78		PDF# 5-453		PDF# 12–88		PDF# 5-622		PDF# 11–675		PDDF# 1-942	
d-value	I/I_o	d-value	I/I_o	d-value	I/I_o	d-value	I/I_o	d-value	I/I_o	d-value	I/I_o	d-value	I/I_o	d-value	I/I_o	d-value	I/Io	d- value	I/Io
-----		-----	---	-----	---	-----	---												
3.34	17	3.36	18	3.34	50	3.34	17												
3.19	20	3.19	20	3.22	35	3.19	20			3.27	52								
2.88	100	2.88	100	2.88	100	2.88	100	2.89	100	2.87	4	2.9	100	2.88	100			2.89	100
2.67	16	2.67	17	-----	---	-----	---	2.7	10			2.69	3	2.66	4	2.67	100	2.68	2
2.40	17	2.40	17	-----	---	2.4	16	2.41	10	2.4	14	2.41	3	2.4	4			2.4	13
-----		-----	---	-----	---	-----	---			2.33	6					2.35	10		
2.19	24	2.19	25	2.19	26	2.19	22	2.19	30	2.19	11	2.2	6	2.19	12	2.18	20	2.19	40
2.01	19	2.02	19	2.01	22	2.01	17	2.02	15			2.02	3	2.01	7			2.02	20
1.80	20	1.80	21	1.80	24	1.78	18					1.81	6	1.8	13			1.8	40
1.78	19	1.78	22	1.78	23	1.78	20	1.8	30	1.76	4	1.79	6	1.78	14				
2.53	15	2.54	16	-----	---	-----	---	2.5	8										
-----	---	-----	---	-----	---	-----	---												
-----	---	-----	---	-----	---	-----	---									5.23	10		
-----	---	-----	---	4.25	27	-----	---			4.21	2								
-----	---	3.69	16	3.69	24	3.68	15	3.7	5							3.68	40	3.71	2
1.54	15	-----	---	1.54	20	1.54	14	1.55	10	1.54	2	1.54	1	1.54	2	1.54	10		
-----	---	-----	---	-----	---	-----	---					1.24	< 1					1.24	2
1.56	14	-----	---	-----	---	-----	---	1.57	8	1.56	4	1.56	< 1	1.56	1	1.55	40	1.55	10
				3.47	22	-----	---												

Table 2 The mole percentage of $CaCO_3$ and the ratio for intensity (I) peaks by using the d_{104}, d_{015} and d_{110} values (see Fig. 3a–g)

Sample# No	d_{104}	d_{015}	d_{110}	I (d_{015})/I (d_{110})	% $CaCO_3$
1 (Jt-1)	2.887	2.533	2.399	0.878	50.33
2 (Jt-8)	2.882	2.533	2.399	0.976	48.66
3 (Jt-13)	2.880	2.540	2.403	0.867	48.00
4 (Jt-15)	2.880	2.540	2.403	0.888	48.00
5 (Jt-16)	2.880	2.540	2.403	0.951	48.00
6 (Jt-17)	2.880	2.533	2.399	0.988	48.00
7 (Jtt-1)	2.878	2.533	2.399	0.849	47.33

they range up to 35% (Fig. 4c). These grains are stained with iron oxides and have no regular boundaries, showing undulose extinction. The microfacies also contain glauconite pellets, which constitute about 10–20%, and occur as sub-rounded to rounded, scattered grains throughout the microfacies. The bioclasts of ostracode constitute about 1% of the grains. The micaceous mineral i.e., muscovite and biotite can be also observed in this microfacies. The microfacies also consist of peloids and ooids (Fig. 4d).

Burrowed sandy ferroan dolomicrites (MJD-2)

The rock is represented by light to brownish grey colored thick-bedded dolomites. This microfacies show fine-grained nature and features such as fenestral fabric porosity, trough cross stratification, and iron leaching. The rhomb size ranges from fine to very fine. The microfacies consist of ferroan dolomites rhombs. The rhombs are anhedral to subhedral having non-planar boundaries. The subhedral rhombs of dolomites are loosely packed whereas anhedral rhombs are tightly packed. The calcites are present in the form of sprites between the rhombs of the dolomites. Iron-oxide staining is common throughout MJD-2 microfacies. The dolomite rhombs constitute 80–90% of the whole composition whereas detrital quartz constitutes about 5–7% (Fig. 5a–d).

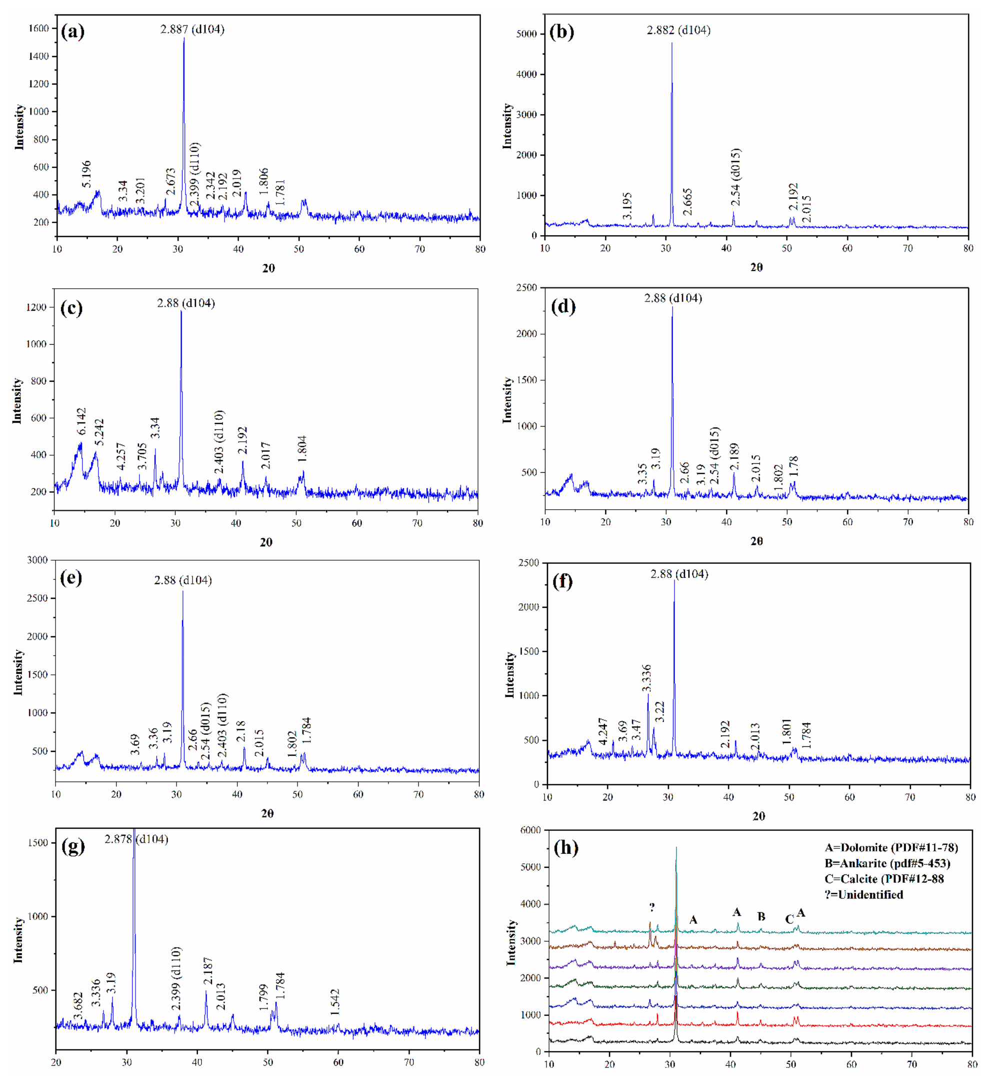

Fig. 3 X-Ray diffraction (XRD) patterns of the analyzed samples. (a) JT-1, (b) JT-8, (c) JT -13, (d) JT -15, (e) JT -16 (f) JT -17, (g) JTT − 1 and (h) showing the combine XRD pattern of a–g samples of Jutana Formation having major phase of dolomite (A) and minor phases of Ankerite (B), Calcite (C)

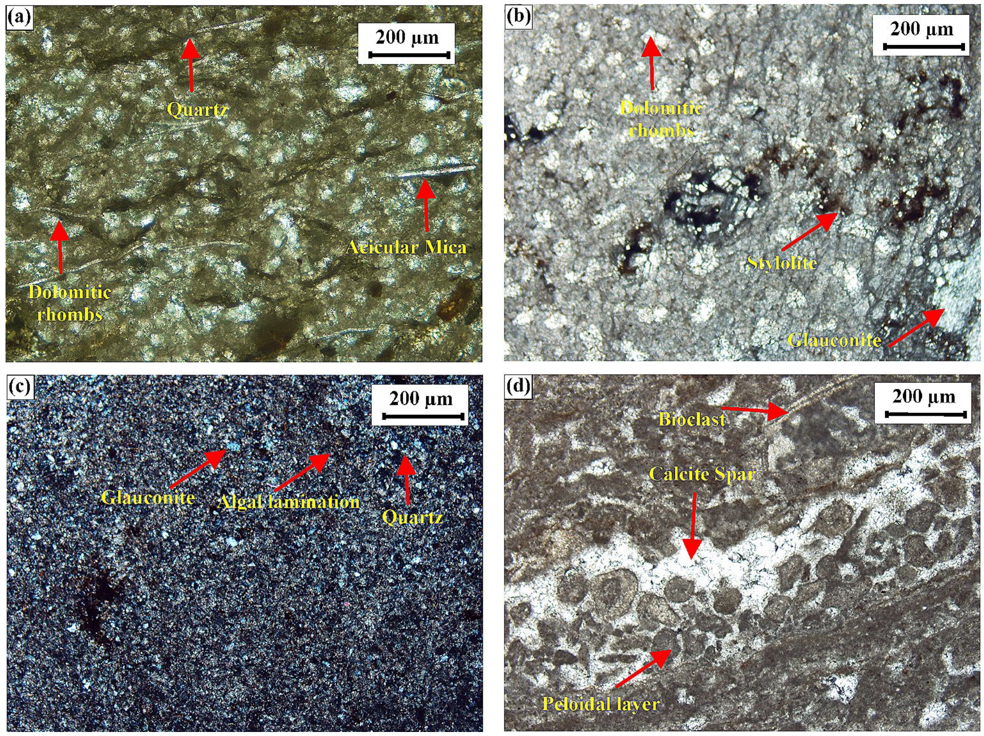

Fig. 4 Microphotographs of algal laminated dolomitic breccia microfacies (MJD-1) of Jutana Formation, under plain polarized light

3 Medium-coarse grained dolomicrite-dolosparite (MJD-3)

At outcrop, the rock is light-grey to yellowish color, thick to thin bedded and has sandy impurities in dolostone. Iron leaching is common at outcrop along the bedding planes. The dolomite rhombs are coarse-grained and well-developed (Fig. 6a). The rhombs are anhedral to subhedral having non-planar boundaries. The quartz grain constitutes $<5\%$ and bioclasts constitute 2%. Heavy minerals (e.g., iron oxide) are present up to 2%. The microfacies possess 5–10% peloidal/ooidal grains, which are dolomitized. Ostracodes, stromatoporoids and bryozoans are also recognized in the microfacies (Fig. 6a–d). The microfacies is stained with iron oxides, possibly due to the stylolite's layers.

Fine grained micaceous dolosparite (MJD-4)

In the outcrop, the rock consists of thick bedded dolomite having light grey to greenish color. This microfacies is composed of very fine-grained dolomite rhombs having a large number of micaceous minerals in acicular/needle shape. The dolomite rhombs are euhedral to subhedral. This microfacies consists of 3% of quartz and about 5–10% mica. Laminations are also present in this microfacies having no fenestral fabric. Stylolites are common along with iron oxide staining. This microfacies is represented by two stages. The first stage is represented by the growth of rhombohedral dolomite and the second stage is represented by diagenetic calcite and micro quartz along the fractures and veins (Fig. 7a–b). The anhydrites can be observed through SEM analysis (Fig. 7c–d).

Mineralogy

The mineralogy of the studied rocks has been identified by X-ray diffraction. The bulk sample of the studied Jutana Formation is composed of major minerals represented by dolomite, calcite, mica and quartz and minor minerals such as glauconite and some opaques (i.e., hematite and magnetite). Quartz is the most important detrital constituent of the Jutana Formation and ranges up to 70% at different stratigraphic levels. There is a gradual change in lithology from the lower part of the succession to the upper part. The lower part is glauconitic with prominent clastic input of siliceous material. The percentage of quartz is greater in the lower part as compared to the middle and upper parts. The middle part of the studied unit is represented by ferroan dolomite. The upper part is purely characterized by the in-situ growth of coarse-grained dolomite.

To verify the mineralogical composition observed at the outcrop and during petrographic studies of Jutana Formation, XRD analyses were performed and the intensity peaks for various minerals were extracted from the XRD analysis. The Jutana Formation exhibits dolomite mineral as a major phase while the calcite and ankerite phases are scarcely distributed (Fig. 3). The molar concentration of $CaCO_3$ in studied samples ranges between 47.33 and 50.33% whereas the

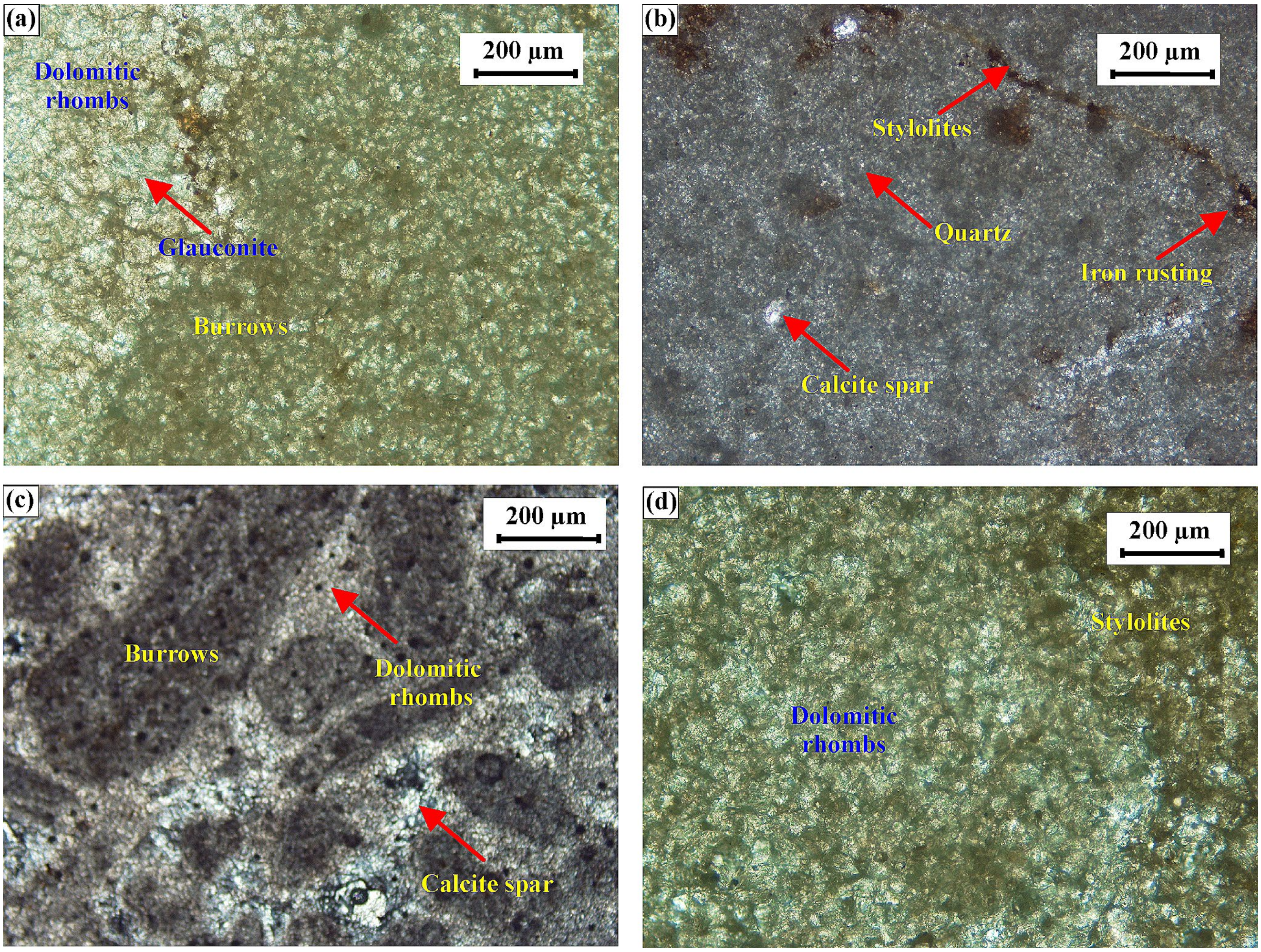

Fig. 5 Microphotographs of burrowed sandy ferroan dolomicrite (MJD-2) of Jutana Formation, under plain polarized light

intensity ratio ranges from 0.849 to 0.988 (Table 1). On one end of the $CaCO_3$ molar concentration is less stoichiometric while on the other it becomes stoichiometric. Similarly, the ordering ranges from less ordering ratio to almost ordered dolomite.

Wireline logging

The petrophysical data in the form of different log suites of the Turkwal-01 well shows similar behavior throughout the Jutana Formation while some changes at the top and bottom along with the contact with other formations is observed. Based on gamma-ray log responses, the Jutana Formation consists of the same lithology in the form of carbonates. However, the value shows variation at both ends, indicating lower and upper contacts of the Jutana Formation (Fig. 8). The lower part consists of thin shale beds followed by subtidal sucrosic dolomites facies, then an intertidal microcrystalline anhydrate dolomite facies, and finally a unit with brecciated beds in the dolomite (Fig. 8). A cross plot was established by Pickett (1977), combining the neutron porosity log and the formation resistivity to show different depositional environments ranging from supratidal to subtidal (Fig. 9).

Discussion

Microfacies of Jutana formation

The MJD-1 microfacies are primarily characterized by algal laminations, indicating a well-oxygenated and agitated environment. These algal laminations commonly occur in the intertidal zone during wet conditions and extend to the subtidal region when there is restricted tidal exchange, leading to high salinity levels and reduced grazing and churning activity. Birdseye structure is common in MJD-1 microfacies, serving as an important indicator of the depositional environment. Modern shallow-marine environments exhibit various forms of birdseye structures, some of which have

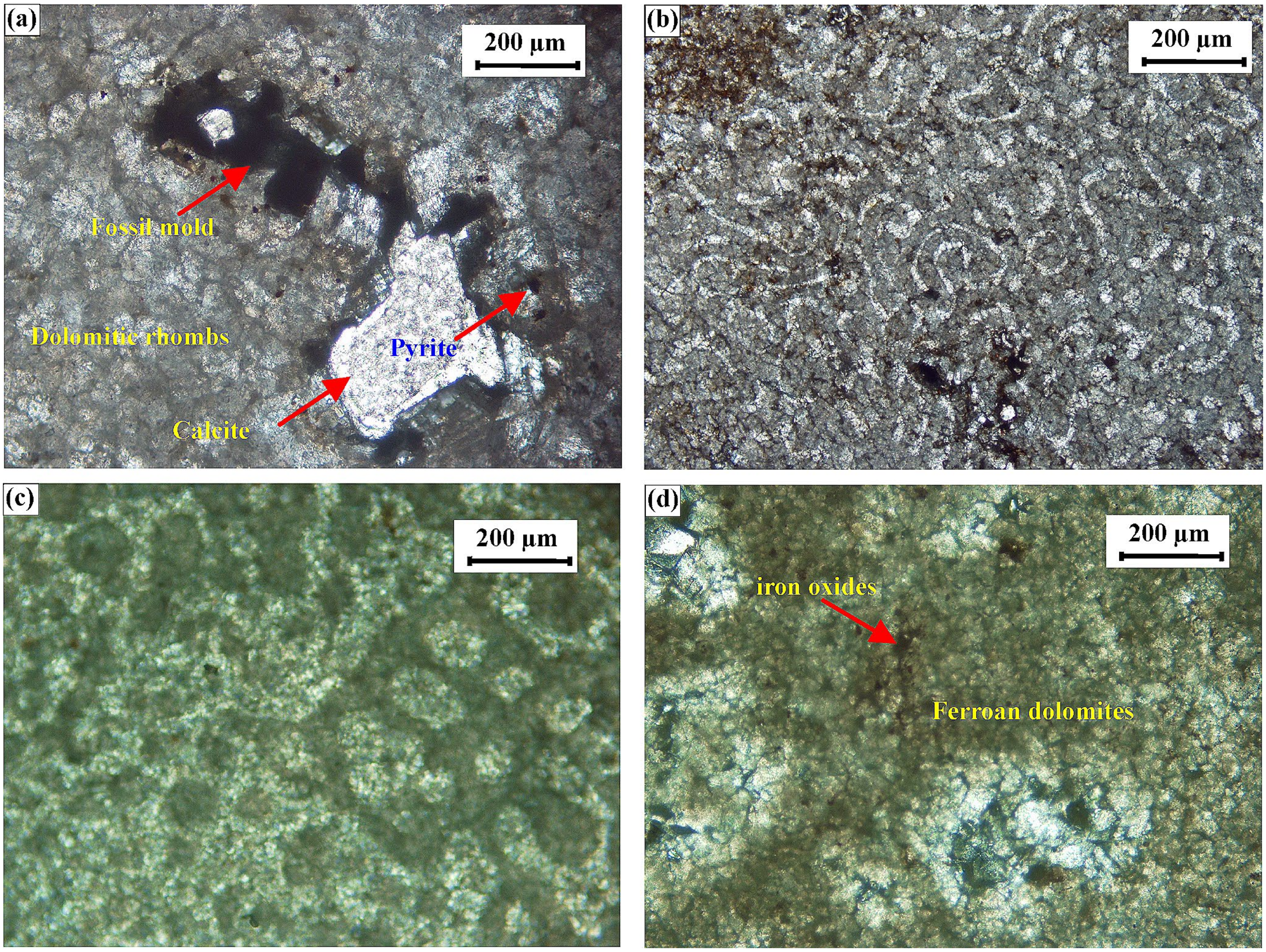

Fig. 6 Microphotographs of In-situ medium-coarse grained dolomicrite-dolosparite (MJD-3) of Jutana Formation, under plain polarized light. (b) Stromatoporoids, (c) Bryozoans

been experimentally confirmed (Shinn 1983). Birdseye structures are found in the modern marine environment in the semi-enclosed lagoon and extended to the subtidal environment (Desheng 1987). The infilling of calcite as a spar in these fenestral pores is characteristic of intertidal and subtidal environments (Wu 1982). The MJD-1 microfacies also display evidence of siliciclastic input, with small, rounded quartz grains suggesting an eolian origin. However, it is noteworthy that oxygenated conditions did not persist throughout the deposition of the lower part of the Jutana Formation, as reflected by the presence of glauconite, indicating a reducing environment during that period. Based on these collective observations, it is reasonable to infer that the rock comprising MJD-1 microfacies were deposited in a subtidal to intertidal environment.

The MJD-2 microfacies exhibit fine-grained nature and features such as fenestral fabric porosity, trough cross stratification, and iron leaching. In barred shorelines within the intertidal zone, water and sediment are carried in the onshore direction by incoming waves, which break over the bars, and in the offshore direction by currents flowing through the rip channels. The barred shorelines display significant dynamism and undergo pronounced seasonal changes. The formation of trough cross stratifications is attributed to fair weather wave base conditions influenced by circulatory cells within barred shorelines (Selley et al. 2005). The presence of quartz indicates the eolian processes while the existence of calcite spar indicates a high-energy carbonate shelf edge environment. The considerable abundance of burrows and pseudocasts further signifies a subtidal to lower intertidal setting. Considering these observations, it is reasonable to infer that the rock of MJD-2 microfacies were deposited within a subtidal environment.

The MJD-3 microfacies display a distinct yellowish color at the outcrop, likely owing to the presence of ferric oxides, particularly hematite, in oxidizing environments (Miall 2004). The iron rusting is further supported through petrographic observations. Additionally, at the outcrop, MJD-3

Fig. 7 Microphotographs of fine grained micaceous cracked sandy dolosparite (MJD-4) of Jutana Formation, under plain polarized light and scanning electron microscope (SEM). (a–b) biotite and muscovite (c–d) SEM microphotographs of MID-4 showing anhydrites

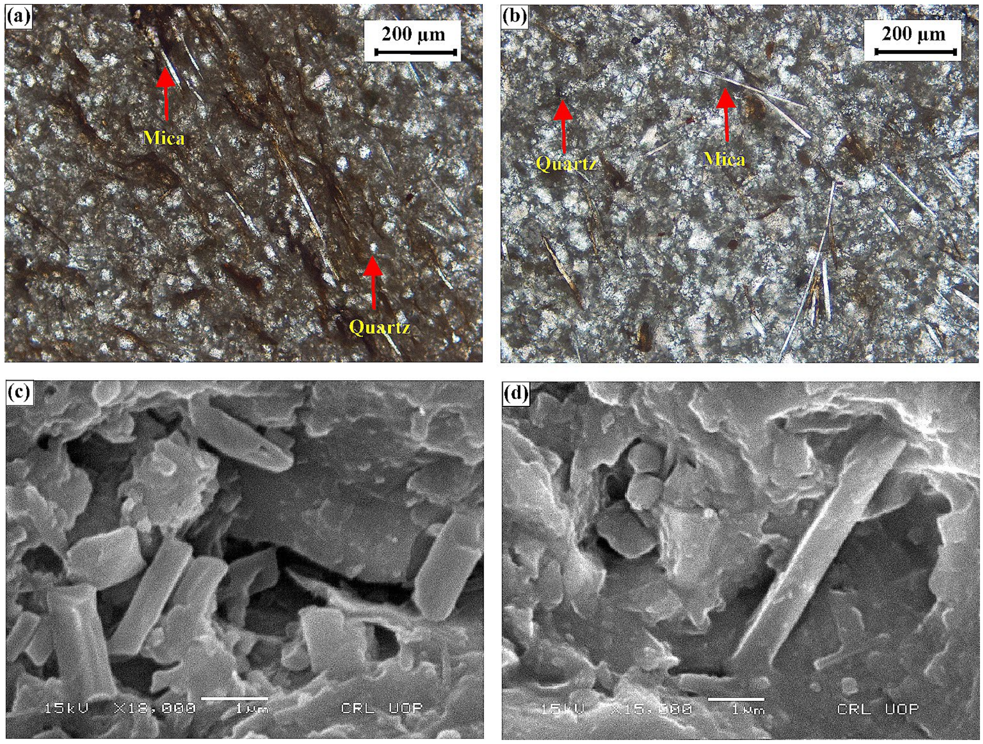

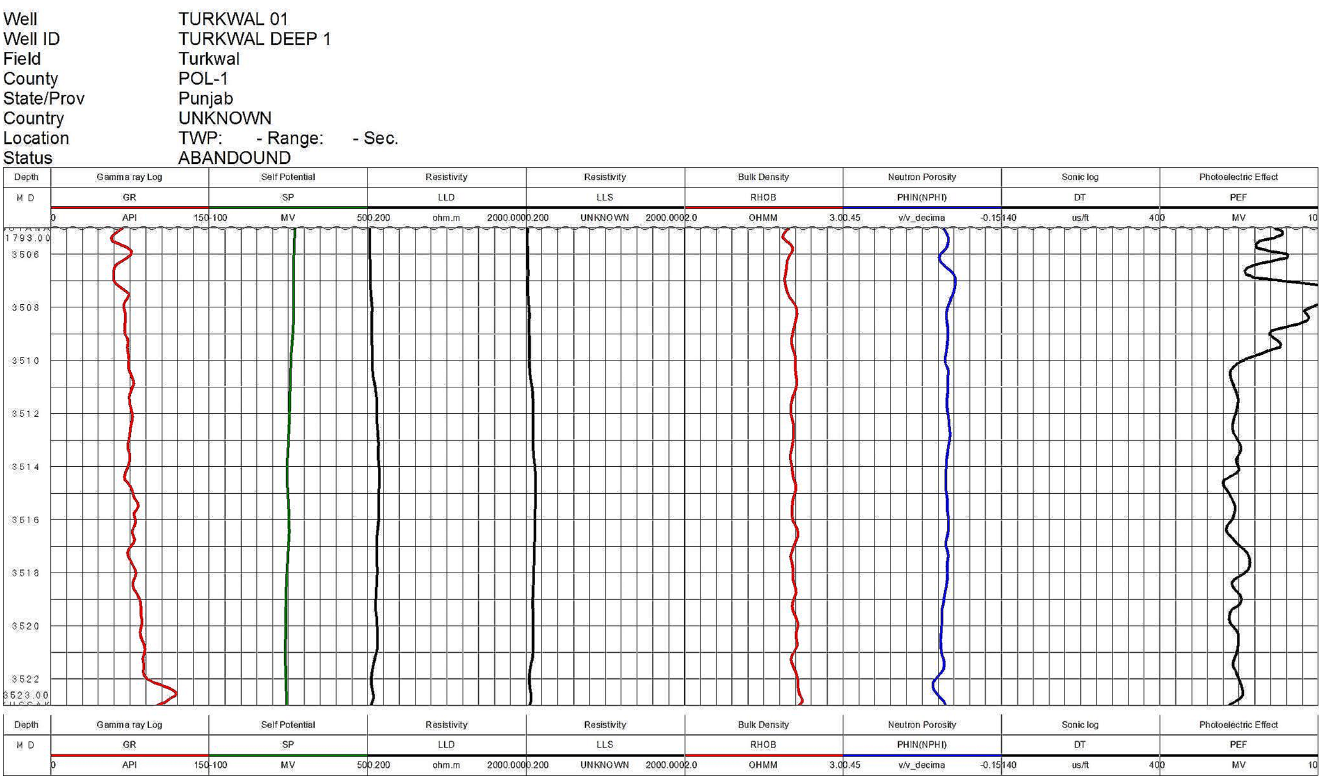

Fig. 8 A full set of wireline logs of Jutana Formation from Turkwal 01 well in Upper Indus Basin, Pakistan

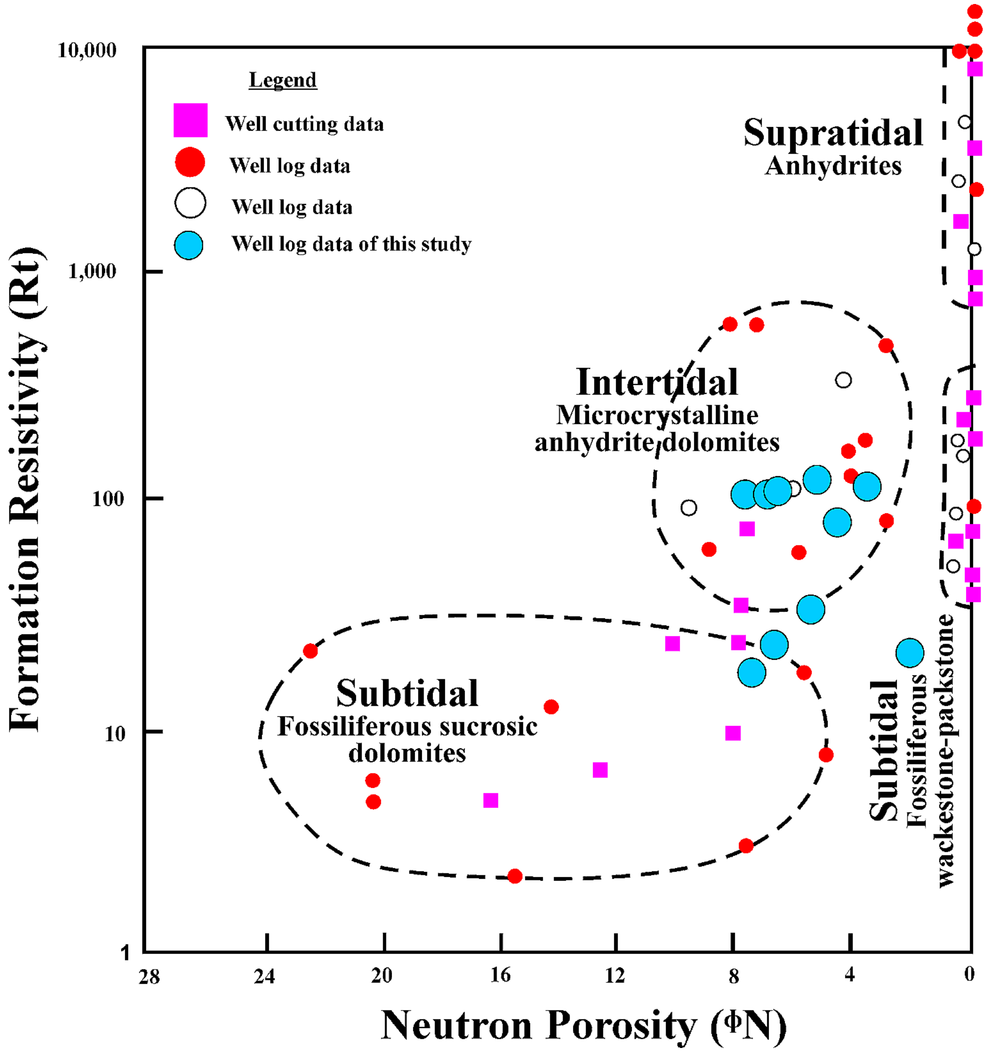

Fig. 9 Cross plot of formation resistivity (Rt) versus neutron porosity (phi N) of Jutana Formation, Upper Indus Basin (after Pickett (1977)

displays channelized beds, which pinch outs at their margins. These channels are the product of tidal actions that narrow towards the land. These channelized beds signify the deposition of tidal creeks within high-energy conditions in the tidal flat setting. The reworked bioclasts are present, potentially transported by ocean currents. Bryozoans and stromatoporoids are observed. Bryozoans, being sessile animals, are typically found in marine environments, predominantly within relatively shallow waters of the continental shelf, spanning from intra-tidal to abyssal depths (Haq and Boersma 1998). The stromatoporoids are exclusively marine organisms, thrive in clear water, well-oxygenated environments and are widespread in shelf and high energy shelf margin settings (Scholle and Ulmer-Scholle 2003). Moreover, the high-energy conditions are reflected by the presence of ooids. These ooids underwent micritization, transforming into pelletoids in protected areas within intertidal and supratidal settings. The existence of pelletoids and ooids indicates a two-phase formation process i.e., initially forming in high-energy conditions before transitioning to low-energy horizons. The field and petrographic observations strongly suggest that the MJD-3 microfacies were deposited within the upper intertidal to supratidal environment.

The microfacies MJD-4 is recognized by a remarkable algal lamination without any disturbances. This specific type of lamination lacks fenestral porosity, a characteristic feature of upper intertidal environments (Tucker 2003). The presence of quartz suggests deposition in an eolian environment, while the origin of the mica can be attributed to digenesis or wind-blown conditions. In microfacies MJD-4, the sedimentary features signify deposition in mixed carbonate and siliciclastic tidal flats and therefore the mica may be detrital or diagenetic in origin i.e., formed from the clays.

Depositional setting of Jutana formation

The detailed outcrop and petrographic observation suggest that the dolomites of the Jutana Formation are primary in nature otherwise secondary. The presence of algal stromatolite, absence of relic features of limestone, chert and pervasive dolomitization indicates the primary nature of dolomites. However, the previous work on the Jutana Formation suggested that laminations are indicative of an absence of any bottom movement of sediments and the prevalence of calm conditions in the depositional basin (Khan et al. 1977). They refer to the lamination as the alternate lamina of mica, quartz and dolomite/calcite. However, they had not noticed the algal lamination and fenestral fabric which are the characteristic features of subtidal to upper intertidal environments having agitated water conditions (Tucker 2003) The depositional setting based on the microfacies analysis and field observation suggested that these dolomites were deposited in the tidal plate environments, but the diagenetic feature makes its primary origin doubtful. Therefore, it is assumed that these were primary in nature but later, the diagenetic process altered its original fabrics. The outcrop and petrographic observation suggest that the Jutana Formation is deposited in a carbonate platform in subtidal, intertidal to supratidal settings (Fig. 10).

Mineralogy and Diagenesis

Dolomite includes a group of carbonate minerals with similar but not identical Mg/Ca ratios and a range of chemical variations and lattice structures (Warren 2000). It constitutes a spectrum of natural Ca-Mg carbonates with chemical compositions closely resembling ideal dolomite. However, these compositions often exhibit weak or diffuse XRD reflections, indicating varying degrees of cation disorder (Hardie 1987). In the ideal form of dolomite, there exist an equal number of Ca and Mg ions, arranged in separate sheets alongside carbonate planes. Nonetheless, natural dolomites deviate from stoichiometry, lacking the ideal molar ratio of $CaCO_3/MgCO_3$ at 50:50. Commonly, they feature an excess of Mg, resulting in a Ca/Mg ratio of 58:42, and less frequently an excess of Ca, reaching up to $Ca_{48}Mg_{52}$ (Wright and Tucker 1990).

Non-stoichiometric dolomites generally demonstrate lower levels of order when compared to “ideal” dolomites, attributed to the presence of some Ca ions in the Mg sheet and vice versa. While it is theoretically feasible for a 50:50 Ca/Mg carbonate to exhibit no ordering reflections if the cation sheets in the lattice consist of equal mixtures of Ca and Mg. All naturally occurring dolomites showcase some degree of order otherwise, the mineral cannot be classified as dolomite. Most modern dolomites display substandard ordering reflections in contrast to many ancient dolomites. At high temperatures (over 100 °C), the amount of disorder increases, and above 1200 °C, complete disorder may exist (Goldsmith and Heard 1961).

In the study of different genetic dolomite groups distinguished by Lumsden and Chimahusky (1980) and Morrow (1982), three primary dolomite groups were identified based on stoichiometry, texture, and the presence or absence of associated evaporites. These groups include (1) coarsely crystalline near-stoichiometric (50.0–51.0 mol %$CaCO_3$) dolomites, (2) finely crystalline Ca-rich (54.0–56.0 mol % $CaCO_3$) dolomites, not associated with evaporites, and (3) finely crystalline nearly stoichiometric (51.0–52.0 mol % $CaCO_3$) dolomites associated with evaporites. Dolomites in Group 1 are typically of late diagenetic burial origin, while the second and third groups are commonly near-surface and early diagenetic. According to the classification of dolomite groups, the molar concentration of the dolomites in the Jutana Formation closely aligns with finely crystalline nearly stoichiometric dolomites associated with evaporites (Lumsden and Chimahusky 1980; Morrow 1982). The ordering of the dolomites in the Jutana Formation increases from the bottom to the top, as evidenced by the ordering ratio of d_{015}/d_{110} increases from 0.878 to 0.988 (Fig. 11).

The Jutana Formation has undergone various diagenetic episodes. The diagenetic features observed during outcrop and petrographic studies include stylolite, fracturing (deformation feature), mechanical compaction, biomoldic porosity, alignment of mica, development of spar and iron leaching. In the diagenetic sequence of carbonates, the stylolite, mechanical compaction and biomoldic porosity usually developed at shallow depths and

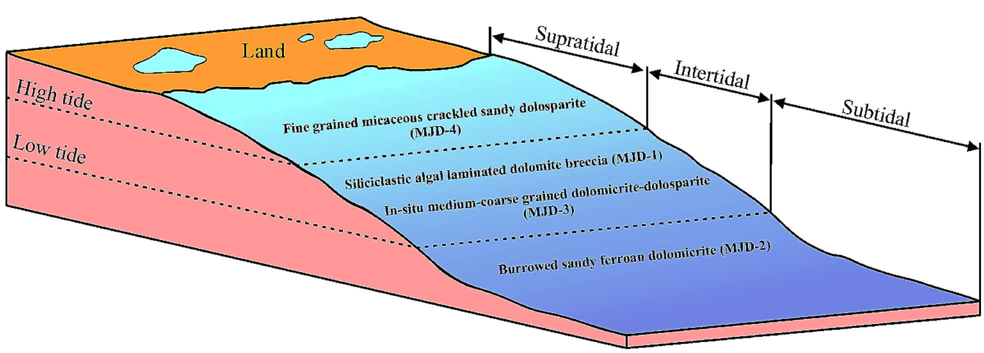

Fig. 10 Depositional modal for the Jutana Formation showing depositional environments of various microfacies identified in present study

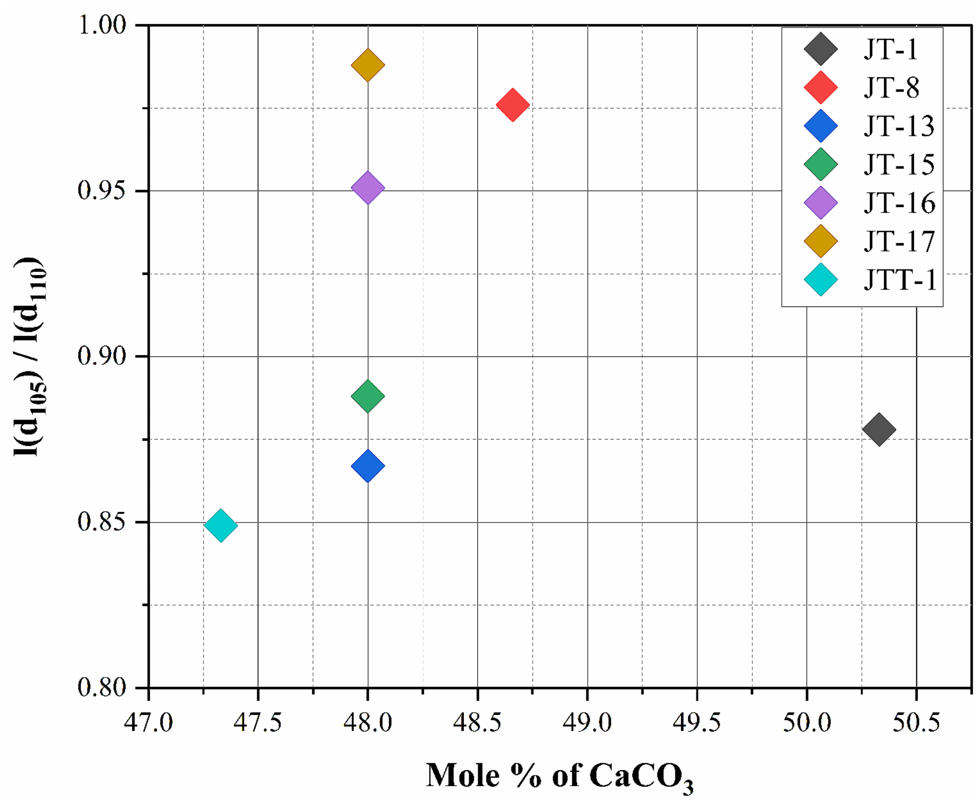

Fig. 11 The degree of order versus stoichiometry of Jutana Formation (XRD samples) (I-integral intensity of XRD peaks)

fracturing developed at deeper depths (Loucks and Longman 1982).

Wireline logs data analysis

The wireline data findings closely align with the results of the petrographic study and XRD analysis for the Jutana Formation. In the petrographic study, the interpretation of different minerals and their associations with specific depositional environments was conducted, leading to the suggestion of intertidal to subtidal environments for the Jutana Formation. The wireline logs data, in turn, reveal a consistent lithological trend, primarily characterized by carbonates. The lower segment features thin shale beds succeeded by subtidal sucrosic dolomites facies, followed by an intertidal microcrystalline anhydrate dolomite facies, and the last unit with the presence of brecciated beds in the dolomites (Fig. 8). Additionally, the logs exhibit abrupt changes near both ends, the idea that the Jutana Formation is interbedded with shale near to its upper contact, while its lower contact exhibits a sharp demarcation with the underlying Kussak Formation. The cross plot of the neutron porosity log and the formation resistivity following Pickett (1977) further confirm the depositional setting of the Jutana Formation (Fig. 9).

Conclusion

The outcrop, petrographic, and geochemical analysis of the Jutana Formation highlights the preservation of an excellent record of both deposition and post-depositional processes. Upon comprehensive analysis and interpretation of the gathered data, the following conclusions have been drawn:

1. The dolomites within the Jutana Formation were originally deposited in a primary nature. However, subsequent diagenesis has obscured many of its primary features, causing doubt about its primary origin.
2. Various facets support the primary nature of dolomites within the Jutana Formation, such as outcrop investigation, petrography, and XRD. Noteworthy outcrop-based characteristics, including a substantial sequence of widespread dolomite, algal laminations, fenestrae, the absence of marine fossils, and internal brecciation, all suggest a primary mode of deposition for the dolomites of Jutana Formation in peritidal environments. Furthermore, the tidal flats feature tidal creeks, evidenced by channelized beds within the Jutana Formation.
3. Microfacies analysis provides additional support for the primary origin of the dolomites of the Jutana Formation, represented by algal laminations under microscopic examination, reworked bioclasts, fenestrae, the

presence of anhydrite under the Scanning Electron microscope, and pervasive dolomitization.

4. XRD analysis indicates that the dolomites of the Jutana Formation are nearly stoichiometric and less ordered. Such dolomites are interpreted as being of early diagenetic origin, forming in upper intertidal to supratidal environments.
5. Data derived from wireline logging closely aligns with previous findings. In this instance, four facies were identified by interpreting cross-plot data obtained from neutron porosity logs and total formation values. The environment for the Jutana Formation is interpreted using cross-plot graphs, indicating a range from subtidal to intertidal.
6. The integration of outcrop, microfacies, XRD analysis, and wireline log data collectively suggests that the Jutana Formation was primarily deposited in peritidal settings, spanning from subtidal to intertidal environments.

Acknowledgements The authors are thankful to University of Peshawar for assistance during field work. The authors are also show deep gratitude to the Institute for Advanced Marine Research, CUG Guangzhou for interpretation and laboratory analysis.

Author contributions M.I, H.R, S.S.H proposed the research work and performed the fieldwork, M.R, and A.K helped the field party in the analysis and interpretations. M.I, H.R, S.S.H prepared the initial draft of the manuscript which is finalized by M.R. All the research work was under the supervision of S.K.

Data availability No datasets were generated or analysed during the current study.

Declarations

Competing interests The authors declare no competing interests.

Conflict of interest There is no financial or ethical conflict of interest among the authors or with any third party.

References

Ahmad N, Ahsan N, Sameeni SJ et al (2013) Sedimentology of the early Middle Cambrian Jutana formation of Khewra area, Eastern Salt Range, District Chakwal, Pakistan. Sci Int 25

Baccelle L, Bosellini A (1965) Diagrammi per la stima visiva della composizione percentuale nelle roccē sedimentarie. Università degli studi di Ferrara

Desheng Y (1987) Bird's-eye structures in carbonate rocks and their environmental significance. AAPG (Am Assoc Pet Geol) bull;(United States) 71

Friedman GM, Sanders JE (1967) Origin and occurrence of dolostones. Developments in sedimentology. Elsevier, pp 267–348

Gee ER (1945) The age of the Saline Series of the Punjab and of Kohat. Proceedings of the National Academy of Science India 14:269–310

Given RK, Wilkinson BH (1987) Dolomite abundance and stratigraphic age; constraints on rates and mechanisms of phanerozoic dolostone formation. J Sediment Res 57:1068–1078

Goldsmith JR, Heard HC (1961) Subsolidus phase relations in the system CaCO3-MgCO3. J Geol 69:45–74

Gregg JM, Bish DL, Kaczmarek SE, Machel HG (2015) Mineralogy, nucleation and growth of dolomite in the laboratory and sedimentary environment: a review. Sedimentology 62:1749–1769

Haq BU, Boersma A (1998) Introduction to marine micropaleontology. Elsevier

Hardie LA (1987) Dolomitization; a critical view of some current views. J Sediment Res 57:166–183

Kadri IB (1995) Petroleum geology of Pakistan. Pakistan Petroleum Limited

Kazmi AH, Jan MQ (1997) Geology and tectonics of Pakistan. (No Title)

Kazmi A, Rana R (1982) Tectonic map of Pakistan. Scale 1:2000000, first edition

Khan S, Shah MM (2019) Multiphase dolomitization in the Jutana formation (Cambrian), Salt Range (Pakistan): evidences from field observations, microscopic studies and isotopic analysis. Geologica Acta 17:1–18

Khan MA, Khan MJ, Alizai SAK (1977) Stratigraphy and petrography of the Jutana Dolomite, Khewra Gorge Khewra, Jehlum District; Punjab: Pakistan. Geol Bull Univ Peshawar 9:43–66

Land LS (1985) The origin of massive dolomite. J Geol Educ 33:112–125

Lippmann F, Lippmann F (1973) Crystal chemistry of sedimentary carbonate minerals. Springer

Loucks RG, Longman MW (1982) Lower cretaceous Ferry Lake Anhydrite. product of shallow-subtidal deposition, Fairway field, east Texas

Lumsden DN, Chimahusky JS (1980) Relationship between dolomite nonstoichiometry and carbonate facies parameters

Miall AD (2004) Empiricism and model building in stratigraphy: the historical roots of present-day practices. Stratigraphy 1:3–25

Morrow DW (1982) Diagenesis 1. Dolomite-Part 1: the chemistry of dolomitization and dolomite precipitation. Geosci Can 9:5–13

Pickett GR (1977) Recognition of Environments and Carbonate Rock Type Identification in Formation Evaluation Manual Unit II, section exploration wells: Oil and Gas Consultants International Inc. International, Inc 4–25

Pina CM, Pimentel C, Crespo Á (2020) Dolomite cation order in the geological record. Chem Geol 547:119667

Qiu X, Wang H, Yao Y, Duan Y (2017) High salinity facilitates dolomite precipitation mediated by Haloferax volcanii DS52. Earth Planet Sci Lett 472:197–205

Rahman MU, Ali F, Hayat M (2016) Diagenetic setting, Dolomitization and Reservoir characterization of late cretaceous Kawagarh formation, Khanpur Dam section, Hazara, Pakistan. Int J Economic Environ Geol 7:64–79

Rahman MU, Ali F, Faisal S et al (2017) The impact of Diagenesis and Dolomitization on the Reservoir Potential of Middle Jurassic Samana Suk formation from Khanpur Dam Section Hazara Basin, Khyber Pakhtunkhwa Pakistan. Int J Econ Environ Geol Vol 8:40–54

Schindewolf OH, Seilacher D (1955) in der Salt Range (Pakistan). Abhandlungen der Mathematisch-Naturwissenschaftlichen Klasse 255

Scholle PA, Ulmer-Scholle DS (2003) A color guide to the petrography of carbonate rocks: grains, textures, porosity, diagenesis, AAPG Memoir 77. AAPG

Selley RC, Cocks LRM, Plimer IR (2005) Encyclopedia of geology. Elsevier Academic

Shah SMI (1977) Stratigraphy of Pakistan

Shah MM, Ahmed W, Ahsan N, Lisa M (2016) Fault-controlled, bedding-parallel dolomite in the middle jurassic samana suk formation in Margalla Hill Ranges, Khanpur area (North Pakistan): petrography, geochemistry, and petrophysical characteristics. Arab J Geosci 9:1–18
Shinn EA (1983) Tidal flat environment. Carbonate depositional environments. American Association of Petroleum Geologists Tulsa, OK, pp 171–210
Sibley DF, Gregg JM (1987) Classification of dolomite rock textures. J Sediment Res 57:967–975
Tucker ME (2003) Sedimentary Rocks in the Field THIRD EDITION
Vasconcelos C, McKenzie JA, Bernasconi S et al (1995) Microbial mediation as a possible mechanism for natural dolomite formation at low temperatures. Nature 377:220–222
Warren J (2000) Dolomite: occurrence, evolution and economically important associations. Earth Sci Rev 52:1–81
Wright VP, Tucker ME (1990) Carbonate sedimentology. Blackwell scientific publications
Wu X (1982) Storm-generated depositional types and associated trace fossils in Lower Carboniferous shallow-marine carbonates of three cliffs Bay and Ogmore-by-Sea, South Wales. Palaeogeogr Palaeoclimatol Palaeoecol 39:187–202